Journal of Environmental Chemical Engineering 8 (2020) 104381

Contents lists available at ScienceDirect

Journal of Environmental Chemical Engineering

journal homepage: www.elsevier.com/locate/jece

Utilization of used polyethylene terephthalate (PET) bottles for the development of ultrafiltration membrane

Samuel P. Kusumocahyo*, Syarifa K. Ambani, Sylvia Kusumadewi, Hery Sutanto, Diah I. Widiputri, Irvan S. Kartawiria

Department of Chemical Engineering, Faculty of Life Sciences & Technology, Swiss German University, Tangerang, 15143, Indonesia

ARTICLE INFO

Editor: Teik Thye Lim

Keywords:
Plastic bottle
Polyethylene terephthalate (PET)
Recycling
Ultrafiltration membrane
Water treatment

ABSTRACT

Polyethylene terephthalate (PET) bottle is commonly used as a single-use packaging for beverages. The recycling of used PET bottles is very important since the huge amount of used PET bottles creates serious environmental concerns. In this work, used PET bottles were utilized as a raw material to develop ultrafiltration membranes by phase inversion technique. The results of this study revealed that lowering the polarity of the non-solvent by using various types of non-solvents, namely water-ethanol, water-*n*-propanol, and water-*n*-butanol, resulted in an increase in the water permeate flux of the membrane. The membranes also exhibited higher water permeate fluxes by increasing the molecular weight and the concentration of the additive for the membrane casting solution. Ultrafiltration experiment using aqueous solution containing Bovine Serum Albumin as a model feed solution showed rejection values of up to 91 %.

1. Introduction

Separation and purification processes using membranes have gained more attention in many industries since membranes can be operated with high selectivity and without the use of heat as required by conventional processes such as evaporation. Various types of membranes such as microfiltration, ultrafiltration, nanofiltration, and reverse osmosis membranes have been widely used in food, beverage, pharmaceutical and chemical industries for various separation and purification processes. These types of membranes are basically pressure-driven membranes which only require electrical pumps to operate the membranes. Pervaporation membranes have also become an alternative method to separate various liquid mixtures since the membranes are able to separate components which are difficult to be separated using thermal separation methods [1–3]. Furthermore, membranes for gas separation have been developed due to their high selectivity and low operation energy [4,5]. Based on the material for membrane preparation, membranes are usually categorized into two main groups, namely polymer (organic) membranes and ceramic (inorganic) membranes. However, recently there are also studies on the development of hybrid organic-inorganic membranes [6,7]. Membranes which are commercially available in the market are mostly made from polymer materials. On the other hand, membranes made from ceramic materials have been receiving increasing attention due their chemical and thermal stability [1,5,8]. Recently, many research studies on ceramic membranes are mostly focusing on the development of membranes for gas separation [9]. However, in terms of production cost, the price of ceramic membranes is usually more expensive than that of the polymer membranes [10].

One of the most popular membranes used in water treatment and waste water treatment processes in industries is ultrafiltration membrane. Ultrafiltration membranes are usually characterized by their molecular weight cut-off (MWCO) which ranges from 300 to 500,000 Da. Commercially available ultrafiltration membranes are mostly made from polymer materials such as cellulose acetate and polysulfone. There are many studies on the use of other polymer materials with the aim to improve the membrane performance [11–13] or to reduce the cost of the membranes [14]. However, to the best of our knowledge, there are only few studies on the use of polyethylene terephthalate (PET) as a polymer material to fabricate ultrafiltration membranes [15]. Studies on the utilization of PET as the main polymer material to develop PET track-etched membranes were reported, and the membranes were tested for direct contact membrane distillation to treat liquid radioactive waste [16,17]. A study on the modification of PET track-etched membranes to reduce protein fouling has also been reported [18].

PET is mostly used as a polymer material to produce packaging for

* Corresponding author at: Department of Chemical Engineering, Faculty of Life Sciences & Technology, Swiss German University, The Prominence Tower Alam Sutera, Jl. Jalur Sutera Barat No. 15, Tangerang, 15143, Indonesia.
E-mail address: samuel.kusumocahyo@sgu.ac.id (S.P. Kusumocahyo).

https://doi.org/10.1016/j.jece.2020.104381
Received 27 May 2020; Received in revised form 29 July 2020; Accepted 9 August 2020
Available online 19 August 2020
2213-3437/

food and beverage products due to its outstanding mechanical properties, high transparency, and good gas-barrier resistance. Nowadays, it is very convenient to use PET bottle as single-use packaging for beverages such as soft drinks, mineral water, teas, juices, etc. However, as a consequence, millions PET bottles are disposed of as waste every day, causing a serious environmental problem due to their non-biodegradability. Many studies reported that only a small part of used plastic bottles is recycled, that means used plastic bottles are mostly disposed of as waste without further treatment or just combusted, creating serious environmental concerns [19,20]. Efforts to recycle used PET bottle have been done to counter the environmental issues [21]. Nowadays, used PET bottles are recycled to produce new bottles through a clean recycling process [20]. Used PET bottles are also recycled to make lower-grade products such as carpets, decorations, etc. However, there are only few studies on the recycling process of used PET bottles to make higher-grade products as reported by Rajesh et al. who prepared ultrafiltration membrane using PET as the polymer material by the phase-inversion technique [15]. In their work, PET and additives were dissolved in m-cresol, and the effect of the additives was studied. However, in the membrane preparation using the phase-inversion technique, different types of solvents and non-solvents are also critical factors which have to be studied.

In this study, used PET bottles were used as a polymer material to develop ultrafiltration membranes by the phase-inversion technique. Different types of solvents to produce miscible casting solutions for the membrane preparation were studied. Further, various types of non-solvents and additives with different molecular weights and concentrations were used to study their effect on the microstructure and the ultrafiltration performance of the membranes. Ultrafiltration experiments were carried out using pure water and an aqueous solution containing Bovine Serum Albumin (BSA) as a model feed solution to study the permeate flux and the rejection of the membranes.

2. Experimental

2.1. Materials

Polyethylene terephthalate (PET) bottles for packaging of drinking water were used as the polymer material of the membrane. These PET bottles were colorless as most bottles for drinking water packaging available in the market are colorless. Fig. 1 shows the chemical structure of polyethylene terephthalate (PET). Phenol (≥ 99 %, molecular weight: 94.11 g/mol), m-cresol (≥ 99 %, molecular weight: 108.14 g/mol) and dimethyl sulfoxide (DMSO, anhydrous, ≥ 99.9 %, molecular weight 78.13 g/mol) were used as the solvents to dissolve PET, and were supplied by Merck, Germany. Polyethylene glycols (PEG) with different molecular weights (Mn: 400 and 4000 g/mol) were used as additives for the polymer membrane, and were also supplied by Merck, Germany. Fig. 2 shows the chemical structure of polyethylene glycol (PEG). Technical grade ethanol (96 %), n-propanol (anhydrous, 99.7 %), and n-butanol (anhydrous, 99.8 %) were all purchased from Merck, Germany, and were mixed with distilled water as the non-solvents for polymer precipitation. Bovine serum albumin (BSA, MW = 66,000 g/mol) was used to test the rejection of the membrane, and was purchased from Merck, Germany. Monosodium phosphate (NaH_2PO_4, ≥ 99 %),

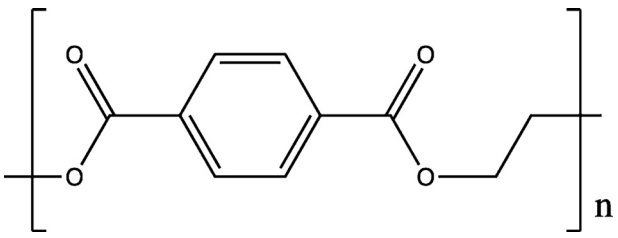

Fig. 1. Chemical structure of polyethylene terephthalate (PET).

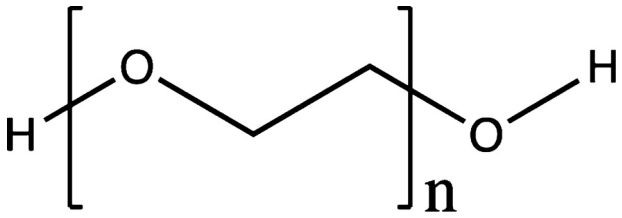

Fig. 2. Chemical structure of polyethylene glycol (PEG).

disodium phosphate (Na_2HPO_4, ≥ 99 %), sodium chloride (NaCl, ≥ 99 %) and potassium chloride (KCl, ≥ 99 %) were used to prepare a phosphate buffered-saline solution for BSA, and were all purchased from Merck, Germany. Distilled and deionized water was used. All chemicals were used as received.

2.2. General scheme of the experiment

Fig. 3 shows the general scheme of the experiment starting from the pre-treatment of the raw material until obtaining the ultrafiltration membranes, and then conducting the membrane characterization.

2.3. Pre-treatment of used PET bottles and preparation of casting solution

Standard laboratory equipment was used for the preparation of the polymer casting solution, namely hotplate (Barnstead Thermolync), beaker glasses, Erlenmeyer flasks, magnetic stirrer, thermometer, volumetric glasses, and analytical balance (Ohaus PA214, USA). First, used PET bottles were collected, then the bottle caps and the labels attached on the bottles were removed. The PET bottles were washed with water, dried at room temperature, and were cut into small pieces with an approximate size of 3 mm x 3 mm. The PET was then dissolved in the solvent (phenol, m-cresol or DMSO) at 100 °C using a hot plate under a continuous stirring using a magnetic bar. Polyethylene glycol (PEG) was dissolved separately in phenol at 100 °C. The composition of the PET, the solvent, and the PEG as the additive is listed in Table 1 below. The PET solution and the PEG solution were mixed together and heated at 100 °C for 1 h using a hot plate under a continuous stirring using a magnetic bar. The polymer solution was then continuously heated at 100 °C without stirring for 10 min to make sure that no air bubbles formed in the solution. PEG was used as additive for the casting solution, since PEG has been known as a plasticizer for polymer films and membranes to improve the flexibility of the polymer films and membranes. PEG also has been known as a pore former that affect the morphology of porous membranes. PEGs with different molecular weights were used to explore the effect of PEG molecular weight on the morphology of the membrane.

2.4. Membrane preparation

Flat sheet PET ultrafiltration membranes were prepared via phase-inversion method. A glass plate with a size of 20cm × 25cm was used for the membrane casting. First, the casting solution was poured onto the glass plate and cast using a home-made casting knife, and then it was immediately immersed in a non-solvent bath containing hydro-alcoholic solution at room temperature (25 °C) for the coagulation process. Based on the preliminary experiment, increasing the temperature of the non-solvent bath above room temperature resulted in membrane defects since phenol diffused rapidly from the polymer matrix into the non-solvent creating defects of the membrane. Various types of water-alcohol mixtures were used as non-solvents, namely water-ethanol, water-*n*-propanol, and water-*n*-butanol mixtures, with a volume ratio of water and alcohol of 1:12 (v/v). After immersing the cast membrane in the non-solvent, phenol was released from the polymer matrix into the non-solvent as phenol was soluble in the non-

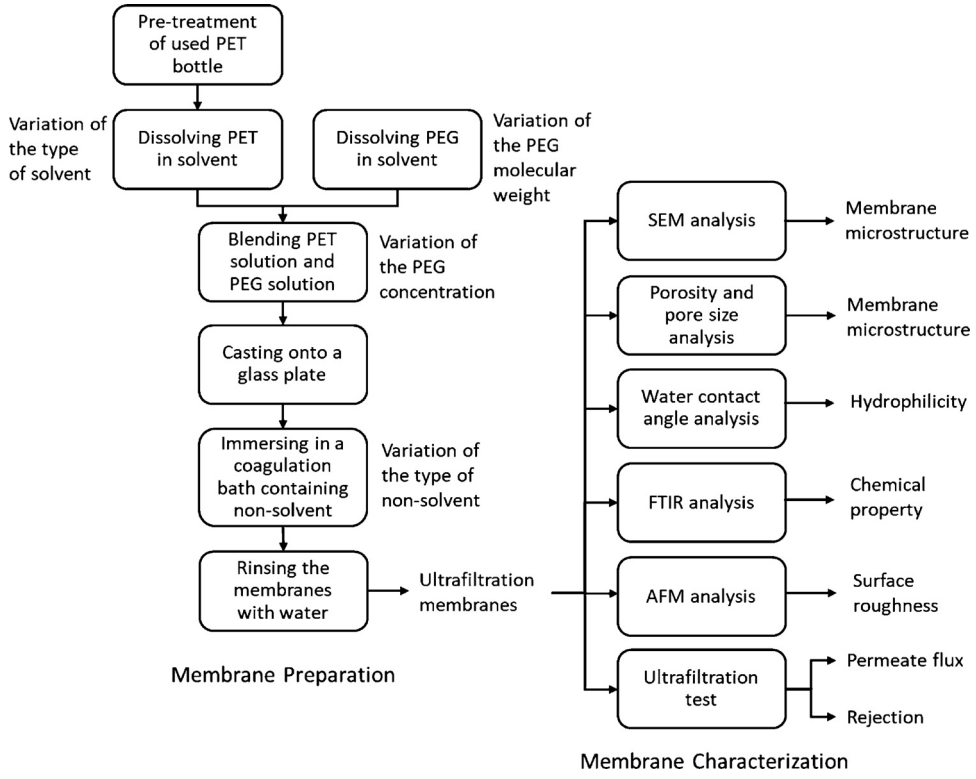

Fig. 3. General scheme of the experiment.

solvent, and the coagulation process occurred. The membranes were then rinsed using distilled water, and stored in a container containing distilled water. Since the non-solvent and the aqueous solution containing phenol are considered as toxic waste, the liquid waste was sent to the third party for waste treatment process to ensure that there is no phenol leaching into the environment. In addition, the purpose of using alcohol in the non-solvent mixture system is to decrease the polarity of the non-solvent mixture. Based on our preliminary experiment, the use of pure water as the non-solvent resulted in a membrane with many defects, because phenol that is highly soluble in water diffused rapidly from the polymer matrix into the water creating defects of the membrane structure. Defects on the membranes were observed visually by placing the membranes on a glass plate equipped with a lighting under the glass, and by using a microscope for small defects. To ensure that the membranes have no defects, all membranes were checked using this visual observation before further use.

2.5. Membrane characterization

The membranes were characterized for their morphology by scanning electron microscopy (SEM, Quanta 650). The membrane samples were fractured in liquid nitrogen prior to SEM evaluation. The thickness of the membranes was measured using a micrometer (Tricle, China). The average thickness was calculated from 5 different positions. The membrane porosity ε was determined by gravimetric method [22,23]. First, the membranes were immersed in deionized water, and the weights of the wet membranes were measured using an analytical balance (Ohaus PA214, USA). The membranes were then dried in an oven at 110 °C for 3 h to completely remove the entrapped water from the membranes. The membrane porosity ε was calculated using the following equation: [22,23]

$$\varepsilon = \frac{(w_1 - w_2)/d_w}{((w_1 - w_2)/d_w) + w_2/d_p} \quad (1)$$

where w_1 is the weight of the wet membrane (g), w_2 is the weight of the dry membrane (g), d_w is the density of water (0.998 g/cm^3), and d_p is the density of the polymer (1.38 g/cm^3). All the reported porosity values were the average values of five replicates.

The mean pore radius r_m was determined using Guerout–Elford–Ferry equation based on the data of porosity and permeation rate of pure water: [22,24,25]

$$r_m = \sqrt{\frac{(2.9 - 1.75\varepsilon) \times 8\eta l Q}{\varepsilon \times A \times \Delta P}} \quad (2)$$

where η is the viscosity of water (8.9×10^{-4} Pa.s), l is the membrane thickness (m), Q is the permeation rate of water (m^3/s), A is the effective membrane area (m^2), and ΔP is the transmembrane pressure (Pa).

Measurement of the water contact angle was conducted to study the

Table 1
Composition of casting solution with different concentrations and molecular weights of PEG as additive.

Membrane Name	PEG concentration (wt%)	PEG molecular weight (Da)	Total polymer concentration (wt%)	Weight ratio		
				PET	Phenol	PEG
Membrane 4000 – 1.25	4.95	4000	20.79	4	20	1.25
Membrane 4000 – 1.5	5.88	4000	21.57	4	20	1.5
Membrane 4000 – 2	7.69	4000	23.08	4	20	2
Membrane 400 – 2	7.69	400	23.08	4	20	2

hydrophilicity of the membranes. The water contact angle on the membrane surface was measured using a contact angle meter (Face CA-D, Kyowa Kaimengaku Co. Ltd, Japan). The contact angle measurement was carried out at 25 °C using deionized water. All the reported values of the water contact angles were the average values of six replicates. Fourier Transform Infrared (FTIR) spectroscopy was conducted using a FTIR spectrometer (Shimadzu IR Prestige-21, Japan) to study the chemical property of the membrane. The membrane was characterized for its surface roughness using Atomic Force Microscopy (Hitachi AFM 5300E, Japan). The AFM measurement was conducted in non-contact mode.

2.6. Ultrafiltration experiment

The ultrafiltration experiment was conducted using a cross-flow membrane cell with an effective membrane area of 51.84 cm^2. The membrane was a flat sheet membrane with a size of 7.2cm × 7.2cm and an average thickness of 249 μm. For the ultrafiltration experiment the membrane was placed on a porous supporting plate equipped in the membrane cell. The feed solution in the feed tank was circulated through the membrane cell using a pump (Masterflex pump, model 07516−00 Cole Parmer, USA), and the permeate was collected in a beaker glass. The schematic diagram of the ultrafiltration experiment set-up is shown in Fig. 4. The ultrafiltration experiment was carried out at room temperature and a pressure of 1 bar. The pressure of 1 bar was chosen to study that the ultrafiltration membranes developed in this work can be operated at a low pressure. Since ultrafiltration membrane is a pressure-driven operation, a low pressure is desired to lower the energy for the pump.

Distilled water was used as the feed to measure the pure water permeate flux of the membrane. The permeate was collected within a certain time interval, and the permeate flux was calculated using the following equation:

$$F = \frac{m}{A\,\Delta t} \tag{3}$$

where the F is the permeate flux given in kg/(m^2h), m is the mass of the permeate (kg), A is the effective area of the membrane (m^2), and Δt is the time interval (h).

To determine the rejection of the membrane, a phosphate buffered-saline solution containing bovine serum albumin (BSA) with a concentration of 1000 ppm was used as a model feed solution for the ultrafiltration experiment. The BSA concentration of 1000 ppm was chosen since it is a typical concentration of the model feed solution to study the rejection of the membrane. BSA is very common to be used as a model of molecule in an aqueous feed solution for ultrafiltration experiment since BSA has a known molecular weight of 66,000 Da which is within the range of the molecular weight cut-off (MWCO) of the ultrafiltration membrane. Since the pore size of the active layer (the surface) of the ultrafiltration membrane is usually too small to be observed by using microscopy instrumentations such as SEM, instead of pore size the ultrafiltration membrane is characterized by its molecular weight cut-off (MWCO), that means the lowest molecular weight of solute in which 90 % of the solute is rejected by the membrane. To prepare the feed solution containing BSA, phosphate-buffered saline was first prepared using the method as described by Hua et al. [26], by dissolving 4.56 g NaH_2PO_4, 23 g Na_2HPO_4, 149.76 g NaCl, and 4.02 g KCl in 1000 mL deionized water. The pH of the phosphate-buffered saline was 6.9 as measured by using a pH meter (Horiba scientific, Laqua PH130). Then BSA was dissolved in the phosphate-buffered saline to obtain an aqueous solution with BSA concentration of 1000 ppm. The ultrafiltration experiment using the BSA solution as the feed was carried out at room temperature and a pressure of 1 bar. The permeate sample was taken after a steady-state condition was achieved. The BSA concentration in the permeate was measured using UV–vis spectrophotometer (PG instrument T-60, UK) at a wavelength of 280 nm, and the rejection of BSA was calculated using following equation:

$$R = \frac{C_F - C_P}{C_F} \times 100\% \tag{4}$$

where R is the rejection (%), C_F is the BSA concentration in the feed solution (ppm) and C_P is the BSA concentration in the permeate (ppm).

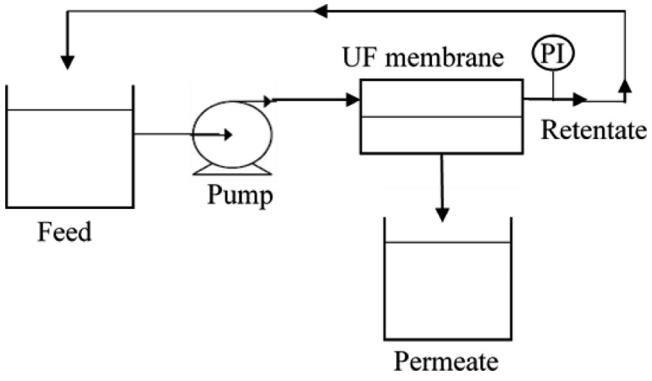

Fig. 4. Schematic diagram of the ultrafiltration experiment set-up.

3. Results and discussion

3.1. Selection of solvent for the casting solution

As the preliminary experiment for the membrane formulation, three different solvents were used to dissolve PET bottle shards, namely phenol, m-cresol and DMSO. These solvents were chosen because pure PET polymer resin is basically soluble in these solvents. It was observed that PET bottle shards could be dissolved in m-cresol at 100 °C, however when PEG was added into the PET solution, an agglomeration was observed in the solution. When DMSO was used as the solvent, it was observed that PET bottle shards could not be completely dissolved in DMSO at 100 °C even after more than 3 h of dissolution process under stirring. On the other hand, both PET bottle shards and PEG could be completely dissolved in phenol at 100 °C. Therefore, for further experiments, phenol was used as the solvent to prepare the casting solution.

3.2. Results of membrane characterization

3.2.1. Effect of type of non-solvent

To study the effect of the type of non-solvent, various types of water-alcohol mixtures were used for the coagulation bath. They were water-ethanol, water-*n*-propanol, and water-*n*-butanol mixtures with a volume ratio of water and alcohol of 1:12 (v/v). PET bottle shards and PEG 4000 were dissolved in phenol as the solvent. After casting the polymer solution onto a glass plate, the cast films were immediately immersed in coagulation baths containing the non-solvents. The average thickness of the membranes was 249 ± 13 μm.

The membranes were then characterized for their microstructures using Scanning Electron Microscopy (SEM). The SEM images of the membrane cross section are shown in Fig. 5 below. The SEM images of the membranes clearly showed that the pores of the membrane cross section became larger by using different non-solvents in the following order: water-ethanol < water-*n*-propanol < water-*n*-butanol, following the decrease in the polarity of the non-solvent. Since phenol was used as the solvent and PEG was used as the additive for the membrane, the molecular interaction between phenol, PEG and non-solvent during the coagulation process strongly affected the formation of the membrane pores. During the coagulation process, phenol interacted with the non-solvent before being released from the polymer matrix and then dissolved in the coagulation bath containing the non-solvent. Due to the low polarity of phenol, the interaction between phenol and non-solvent

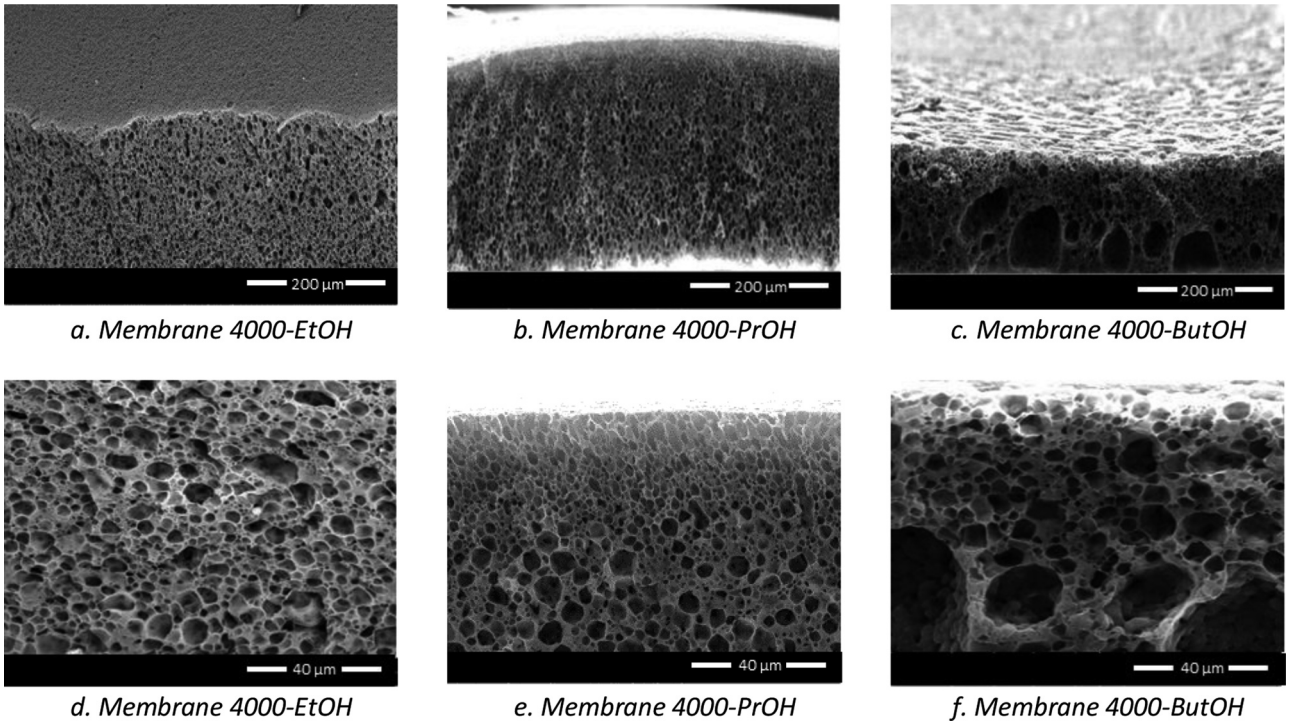

Fig. 5. SEM images of the membranes with different non-solvents (left: water-ethanol, middle: water-*n*-propanol, right: water-*n*-butanol, a,b,c: surface and cross section, d,e,f: cross section).

Table 2
Porosity and mean pore radius of the membranes prepared using different types of non-solvents.

Membrane	Non-solvent	Porosity (%)	Mean pore radius (nm)
Membrane 4000-EtOH	Water-ethanol	75.7 ± 0.2	5.9 ± 0.7
Membrane 4000-PrOH	Water-n-propanol	76.6 ± 0.5	11.1 ± 0.6
Membrane 4000-ButOH	Water-n-butanol	77.2 ± 0.4	13.9 ± 1.6

became stronger in the following order: water-ethanol < water-*n*-propanol < water-*n*-butanol, creating an increase in the pore size of the membrane cross section. On the other hand, the active layer (or the surface) of the ultrafiltration membrane was a smooth layer as observed by using SEM. Since the pore size of the active layer was too small to be observed by using SEM, the mean pore radius of the active layer was determined based on the porosity data and the permeation rate of water. The membrane porosity as determined using the gravimetric method and the mean pore radius are listed in Table 2. As can be seen, the porosity and the mean pore radius also increased in the following order: water-ethanol < water-*n*-propanol < water-*n*-butanol.

3.2.2. Effect of molecular weight of PEG as additive

In order to study the effect of molecular weight of the additive on the membrane microstructure, PEG 400 and PEG 4000 were used as the additives for the membrane preparation. Water-ethanol mixture (1:12 v/v) was used as the non-solvent for both membranes. It was observed that the addition of PEG in the casting solution was important to improve the flexibility of the PET membrane. Without the addition of PEG, the PET membrane was stiff and could not be used for ultrafiltration experiment. It has been known that PEG acts as a plasticizer for various polymer films such as gelation film, poly(arylene ether sulfone) film, and other polymeric films, improving the flexibility of the films [27,28]. Thus, the flexibility of the PET membrane developed in this work was improved by the addition of PEG since PEG acts as a plasticizer for the membrane. Moreover, the addition of PEG increased the hydrophilicity of the membrane as observed through the water contact angle measurement. As can be seen in Table 3, the water contact angle

Table 3
Effect of molecular weight of PEG on the water contact angle of the membranes.

Membrane	Additive	Water Contact Angle (°)
Membrane PET	No PEG	65.5 ± 1.4
Membrane 400−2	PEG 400	63.5 ± 1.1
Membrane 4000−2	PEG 4000	56.5 ± 2.6

of the PET membrane without the addition of PEG was 65.5°, whereas lower water contact angles of 63.5° and 56.5° were observed for the PET membranes containing PEG 400 and PEG 4000, respectively. Fig. 6 shows some examples of the photographs of the water contact angles on the membrane surfaces.

The membranes were then analyzed for their morphology using SEM as shown in Fig. 7. The SEM images showed that the pore size of the cross section of the membrane using PEG 4000 as the additive was higher than that using PEG 400 as the additive. Thus, bigger pores were formed when PEG of high molecular weight was used. Similar phenomenon was also reported by Wongchitphimon et al. who prepared polyvinylidene fluoride-co-hexafluropropylene membranes using PEG as additive [29]. Idris et al. who prepared polyether sulfone membranes using PEG as additive also reported that membranes with PEG of higher molecular weights had larger pores [30]. The pore size of the active layer was then determined based on the porosity and the permeation rate of water, and the data are listed in Table 4. It can be seen that the mean pore radius of the active layer of the membrane prepared using PEG 4000 as the additive was larger than that of the membrane prepared using PEG 400.

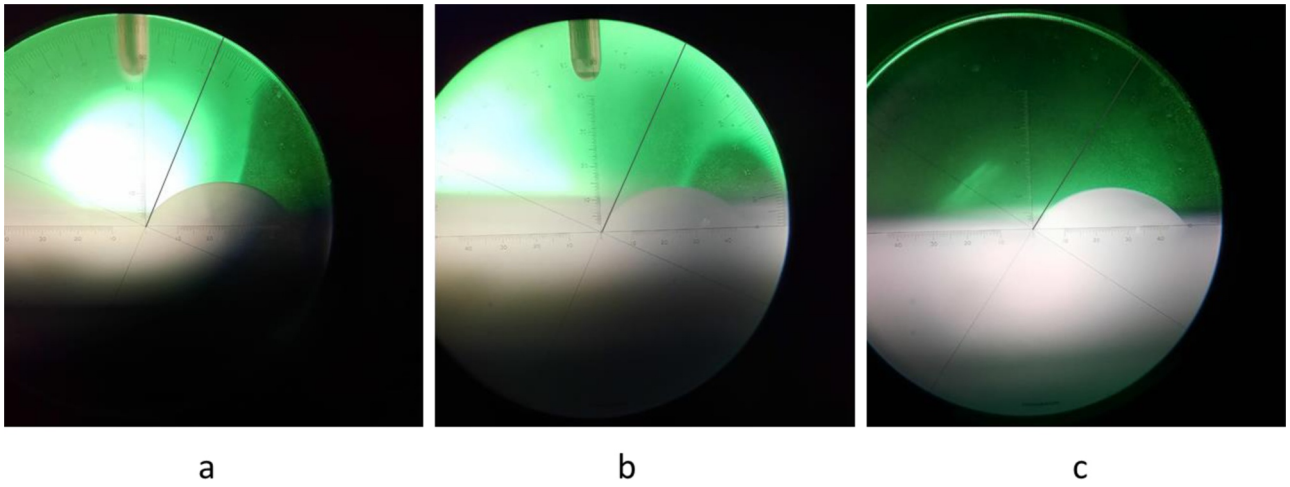

Fig. 6. Photographs of the water contact angles on the membrane surfaces (a: PET membrane without PEG, b: PET membrane with PEG 400, c: PET membrane with PEG 4000).

3.2.3. *Effect of concentration of PEG as additive*

Furthermore, the concentration of PEG in the casting solution was varied with the aim to study its effect on the morphology and the hydrophilicity of the membrane. Water-ethanol mixture (1:12 v/v) was used as the non-solvent, whereas PEG 4000 was used as the additive for all membranes. Table 5 depicts the result of the water contact angle measurement on the membrane surface. As can be seen, the increase in the PEG concentration resulted in an increase in the hydrophilicity of the membrane. Since PEG is a hydrophilic compound, the membrane exhibited a higher hydrophilicity when more PEG was added into the membrane casting solution.

The SEM images of the microstructure of the membranes showed that the increase in the PEG concentration resulted in an increase in the pore size of the membrane cross section as shown in Fig. 8, since PEG acts as pore former [31]. The membrane porosity and the pore size of the active layer are listed in Table 6. As can be seen, the increase in the

Table 4
Effect of molecular weight of PEG on the porosity and the mean pore radius.

Membrane	Additive	Porosity (%)	Mean pore radius (nm)
Membrane 400 – 2	PEG 400	77.5 ± 0.5	10.1 ± 1.8
Membrane 4000 – 2	PEG 4000	81.3 ± 0.0	15.9 ± 3.1

Table 5
Effect of concentration of PEG on the water contact angle of the membranes.

Membrane	PEG concentration (wt%)	Water Contact Angle (°)
Membrane 4000 – 1.25	4.95	62.8 ± 1.2
Membrane 4000 – 1.5	5.88	61.5 ± 0.5
Membrane 4000 – 2	7.69	56.5 ± 2.6

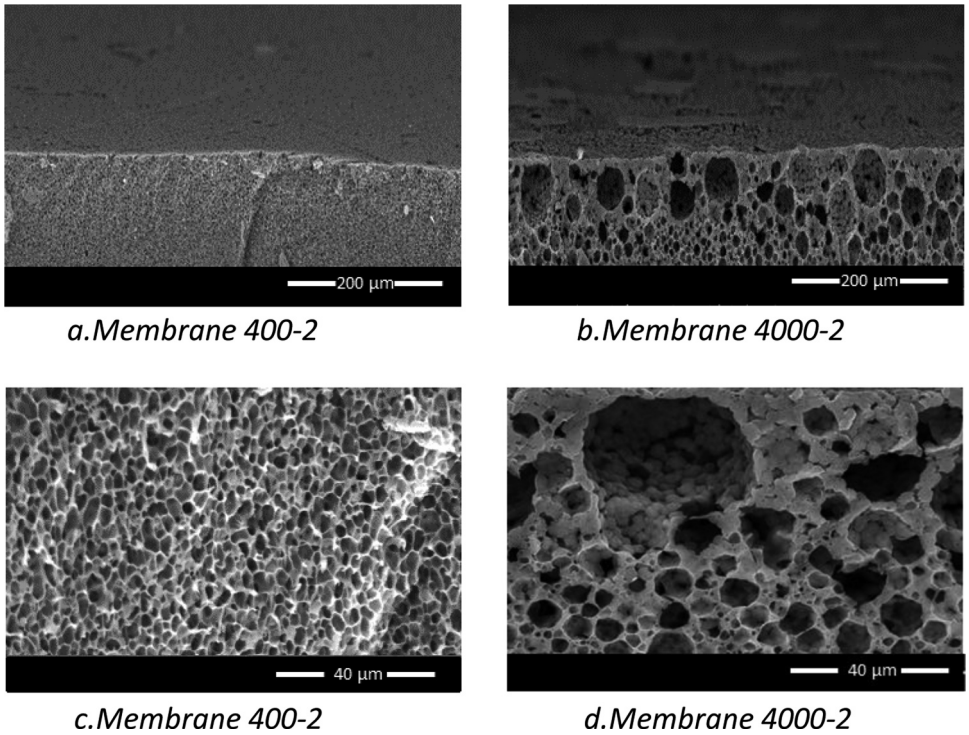

Fig. 7. SEM images of the membranes with different PEG molecular weights (left: PEG 400, right: PEG 4000, a,b: surface and cross section, c, d: cross section).

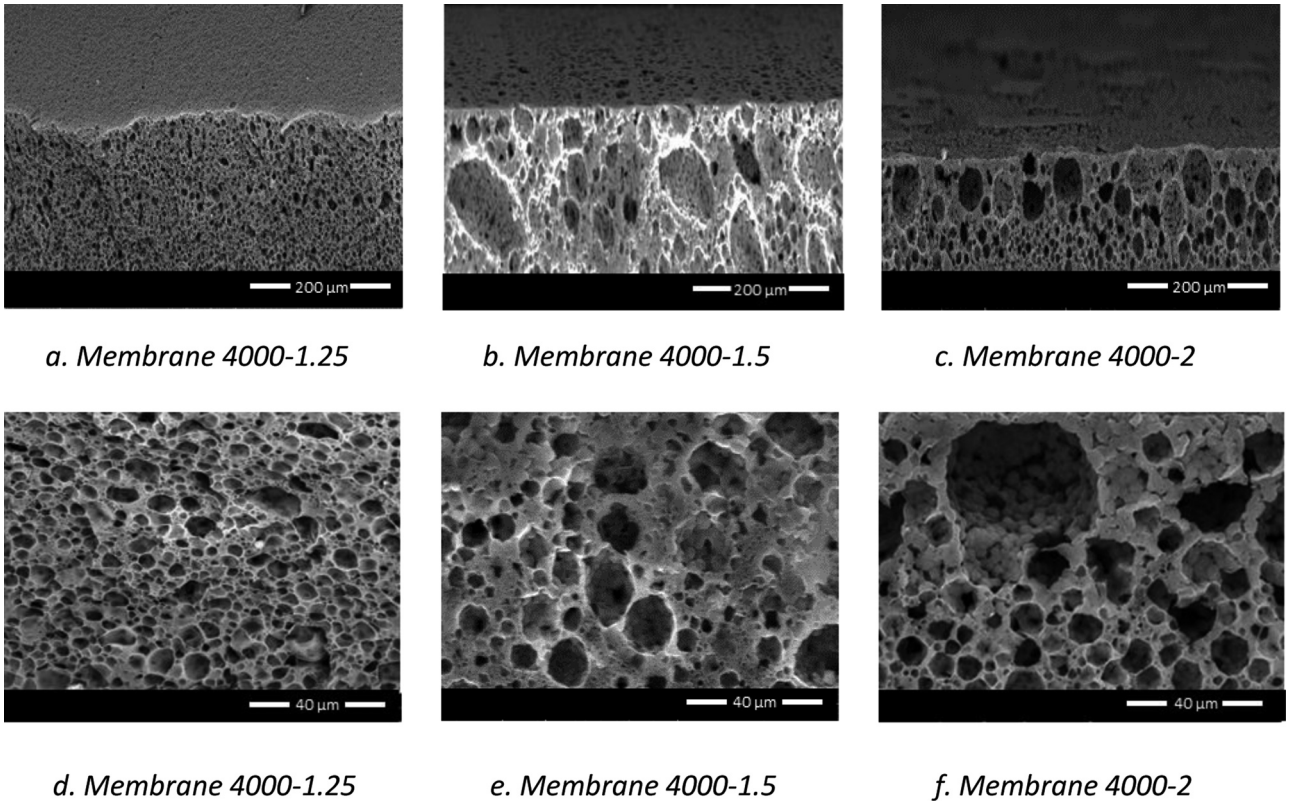

Fig. 8. SEM images of the membranes with different concentrations of PEG 4000 as additive (a,b,c: surface and cross section, d,e,f: cross section).

PEG concentration resulted in the increase in the porosity and the mean pore radius of the membrane. Thus, the porosity and the pore size of the membrane could be controlled by varying the concentration of the PEG as the additive.

3.2.4. FTIR spectra of the membrane

Fig. 9 shows the FTIR spectra of the ultrafiltration membrane prepared from used PET bottle using PEG as the additive. FTIR spectra over wave numbers of 4000 – 400 cm^{-1} are presented. All membranes prepared in this work showed typical spectra of PET films as reported by other studies [32,33]. The peaks at 3054 cm^{-1} and 1578 cm^{-1} were associated with the C–H bond of the phenyl ring of the PET, while the peaks at 2967 cm^{-1} and 737 cm-1 were due to the C–H bond of the ethyl group of the PET. The peaks at 2907 cm^{-1} and 1742 cm^{-1} were assignable to the CO═ bond of the ester group of the PET. Furthermore, the peak at 1408 cm^{-1} was associated to the CC─ bond of the phenyl ring, and the peak at 1140 cm^{-1} was due to the CO─ bond of the PET.

3.2.5. AFM image of the membrane surface

Measurement of the surface roughness of the membrane is crucial to study fouling during ultrafiltration that causes a permeate flux decline with the time. The fouling problem occurs due to the concentration polarization of the particle on the membrane surface. In this work, the surface of the membrane was characterized using Atomic Force Microscopy (AFM) to study the surface roughness. Fig. 10 shows an example of the AFM image of the ultrafiltration membrane prepared from used PET bottle using PEG as the additive. The surface of the membrane showed a typical nodular (hills and valleys) morphology. The mean surface roughness (R_a) and the root-mean-squared surface roughness (R_q) of the membrane was 232.4 nm and 310.7 nm, respectively, as quantified by the AFM software. The height difference between the highest peak and the lowest valley (R_z) was 2067 nm. The surface roughness of this membrane is higher than that of other ultrafiltration membranes made from other polymers such as polyvinylidene fluoride (PVDF) and polysulfone [24,34].

3.3. Results of ultrafiltration experiment

3.3.1. Effect of type of non-solvent on the ultrafiltration performance

The membranes were then tested for their water permeate flux through an ultrafiltration experiment at a pressure of 1 bar at room temperature. Fig. 11 shows the water permeate fluxes of the membranes as a function of the permeation time and the type of non-solvent. As can be seen, all membranes showed a decrease in the water permeate flux with the permeation time, but then became stable after about 50 min of permeation time. This is due to the compaction of the freshly prepared membrane during the pressure-driven permeation experiment. Similar phenomenon was also observed in other polymer membranes as reported by many studies [35,36]. Interestingly, the use of different types of nonsolvent resulted in different water permeate fluxes as can be seen in Fig. 11. The permeate flux of the membrane prepared using water-ethanol as the non-solvent was very low, however a higher

Table 6
Effect of concentration of PEG on the porosity and the mean pore radius.

Membrane	PEG concentration (wt%)	Porosity (%)	Mean pore radius (nm)
Membrane 4000 – 1.25	4.95	75.7 ± 0.2	5.9 ± 0.7
Membrane 4000 – 1.5	5.88	78.1 ± 0.3	11.5 ± 2.8
Membrane 4000 – 2	7.69	81.3 ± 0.0	15.9 ± 3.1

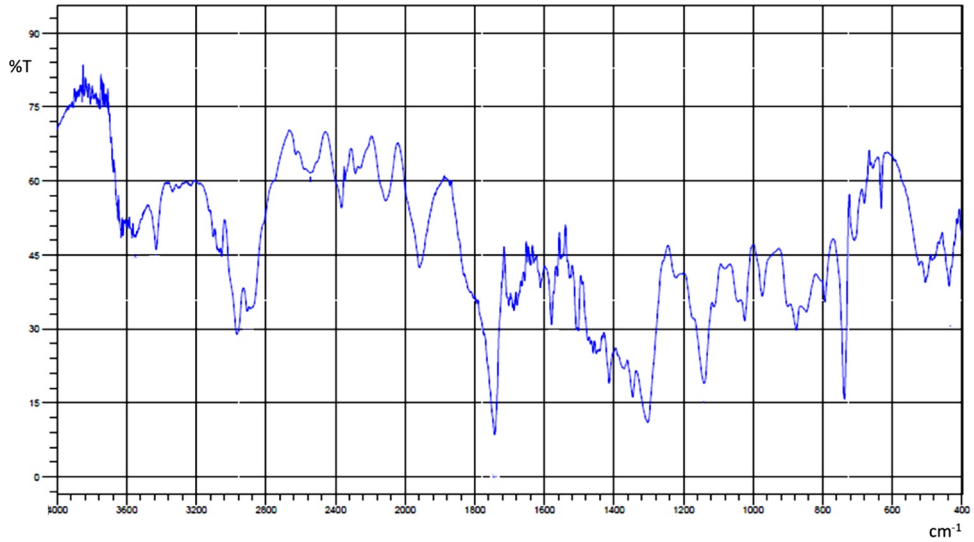

Fig. 9. FTIR spectra of the membrane.

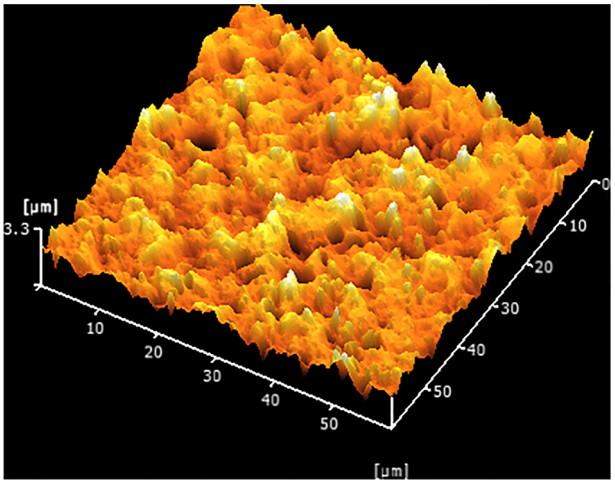

Fig. 10. AFM image of the membrane surface.

permeate flux was obtained when water-*n*-propanol was used as the non-solvent for the membrane preparation. The highest permeate flux was achieved by the membrane prepared using water-*n*-butanol as the non-solvent. Thus, the permeate flux increased in the following order: water-ethanol < water-*n*-propanol < water-*n*-butanol. This result is in accordance with the result of the membrane microstructure as observed using SEM and the result of the porosity and pore size analysis as described previously. The increase in the pore size of the cross section of the membrane resulted in an increase in the pore size of the active layer (the membrane surface), thus an increase in the permeate flux.

Furthermore, the ultrafiltration experiment was conducted using an aqueous solution of phosphate buffered-saline containing 1000 ppm Bovine Serum Albumin (BSA) as the model feed solution to study the ability of the membranes to reject the BSA molecule that has a molecular weight of 66,000 Da. Table 7 depicts the effect of type of non-solvent on the rejection of BSA molecules. It can be seen that the membrane prepared using water-ethanol as the non-solvent exhibited the highest BSA rejection of 90 %, which means that the molecular weight cut-off (MWCO) of the membrane is 66,000 Da. However, the membrane prepared using water-*n*-propanol as the non-solvent exhibited a lower rejection of 87 %, whereas that using water-*n*-butanol showed the lowest rejection of 61 %. This result is also in accordance with the result of the water permeation experiment, the analysis of the membrane microstructures using SEM, and the analysis of the porosity and pore size as described above. The rejection of the membrane decreased when the membrane was prepared using the non-solvent in the following order: water-ethanol > water-*n*-propanol > water-*n*-butanol, because of the increase in the pore size of the membrane.

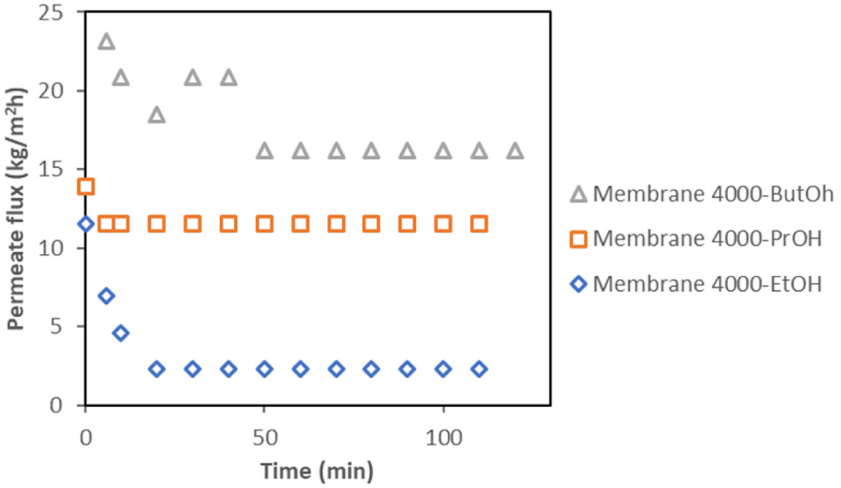

Fig. 11. Effect of type of non-solvent on the water permeate flux.

Table 7
Effect of type of non-solvent on the rejection of BSA molecules.

Membrane	Non-solvent	Rejection (%)
Membrane 4000-EtOH	Water-ethanol	90
Membrane 4000-PrOH	Water-n-propanol	87
Membrane 4000-ButOH	Water-n-butanol	61

In the ultrafiltration experiment using the aqueous solution containing BSA as the feed solution, a decrease in the permeate flux with time was observed as can be seen in Fig. 12. The permeate flux decline with time was caused by membrane fouling due to the concentration polarization of BSA molecules on the membrane surface. The fouling occurred as the membrane showed a relatively high surface roughness as observed by AFM above, and it caused an accumulation of BSA molecules on the membrane surface.

3.3.2. Effect of molecular weight of PEG on the ultrafiltration performance

The membranes prepared using different molecular weights of PEG as the additive were then characterized for their ultrafiltration performance using pure water as the feed solution. The result of the permeation experiment using pure water is shown in Fig. 13. As can be seen, the permeate flux of the membrane using PEG 4000 as the additive was higher than that using PEG 400 as the additive. This result is also in accordance with the result of the microstructure analysis using SEM, the result of the hydrophilicity analysis using water contact angle measurement, and also the porosity and pore size analysis as described above. The permeate flux of the membrane using PEG 4000 was higher than that of the membrane using PEG 400 as the additive because of the larger pore size and the higher hydrophilicity. The membranes using PEG 400 and PEG 4000 as the additives also showed a decrease in the water permeate flux with the time before a stable permeate flux was reached because of the compaction of the freshly prepared membrane during the pressure-driven permeation experiment [35,36].

Moreover, the ability of the PET membrane to reject BSA molecules was studied through an ultrafiltration experiment using an aqueous solution of phosphate buffered-saline containing 1000 ppm Bovine Serum Albumin (BSA) as the model feed solution. The results are listed in Table 8 which shows that the membrane prepared using PEG 400 exhibited a high rejection of 91 %, while that using PEG 4000 exhibited a lower rejection of only 30 %. Thus, the use of low molecular weight of PEG resulted in a high rejection but a low permeate flux due to the small pore size of the membrane. Fig. 14 shows the permeate fluxes of the membranes during the ultrafiltration experiment using the aqueous solution containing BSA as the feed solution. The decline of the permeate flux with the time was caused by membrane fouling as described previously. In the ultrafiltration of the aqueous BSA solution, the permeate flux of the membrane 4000 – 2 was also higher than that of the membrane 400 – 2.

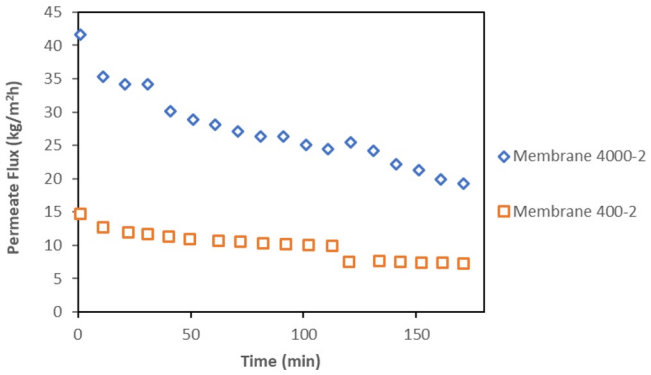

Fig. 13. Effect of molecular weight of PEG as additive on the water permeate flux.

Table 8
Effect of molecular weight of PEG as additive on the rejection of BSA molecules.

Membrane	MW of PEG (Da)	Rejection (%)
Membrane 4000 – 2	4000	30
Membrane 400 – 2	400	91

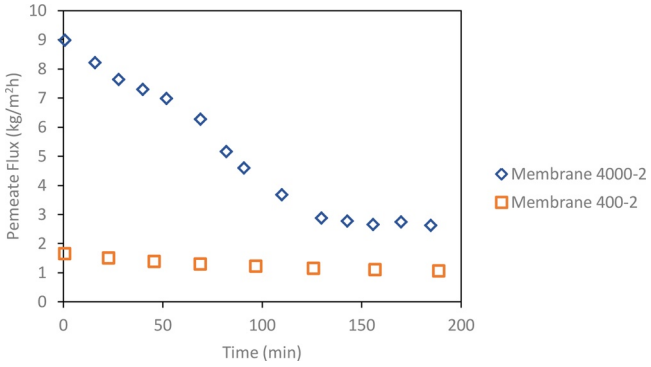

Fig. 14. Effect of molecular weight of PEG as additive on the permeate flux using an aqueous solution containing BSA as the feed.

3.3.3. Effect of concentration of PEG on the ultrafiltration performance

Fig. 15 shows the water permeate flux of the membranes prepared

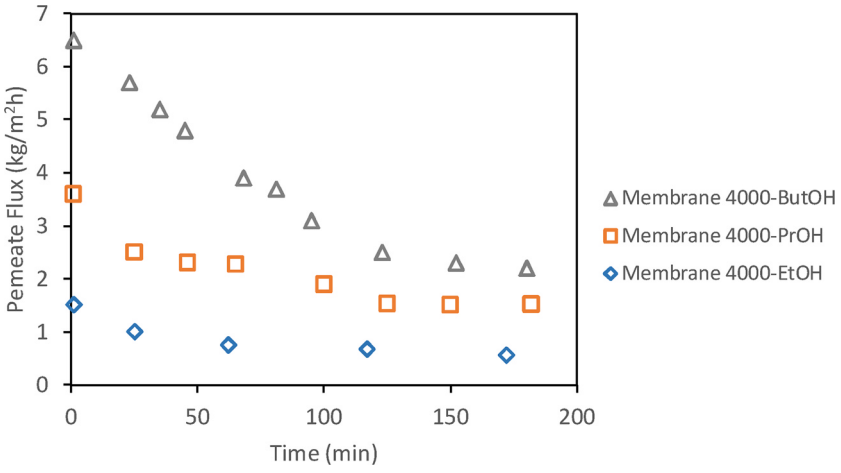

Fig. 12. Effect of type of non-solvent on the permeate flux using an aqueous solution containing BSA as the feed.

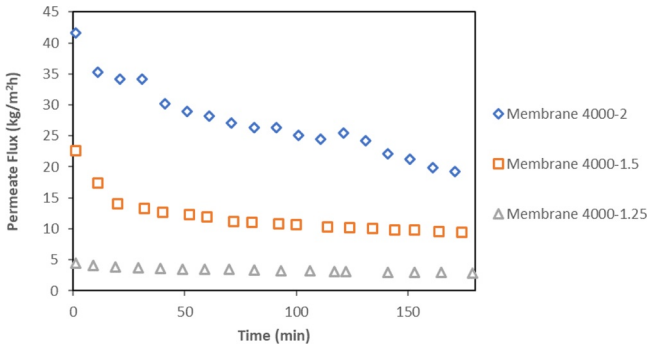

Fig. 15. Effect of concentration of PEG as additive on the water permeate flux.

Table 9
Effect of concentration of PEG as additive on the rejection of BSA molecules.

Membrane	PEG concentration (wt%)	Rejection (%)
Membrane 4000 – 1.25	4.95	90
Membrane 4000 – 1.5	5.88	68
Membrane 4000 – 2	7.69	30

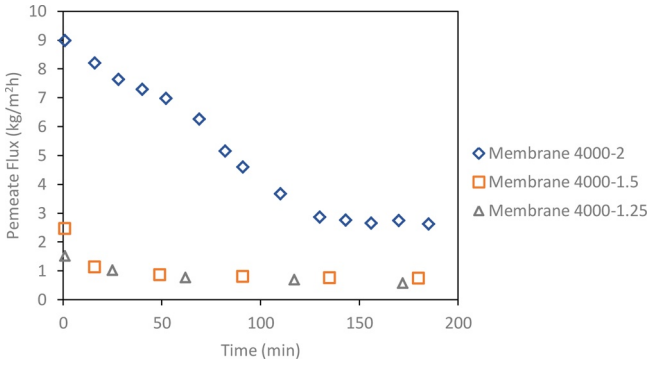

Fig. 16. Effect of concentration of PEG as additive on the permeate flux using an aqueous solution containing BSA as the feed.

using different PEG concentrations. It can be seen that the increase in the PEG concentration of the membrane resulted in an increase in the water permeate flux because of the increasing pore size of the membrane as described above. Moreover, since PEG remained in the PET polymer matrix, the higher concentration of PEG in the polymer matrix increased the hydrophilicity of the membrane as described previously, and therefore increasing the water permeate flux. The BSA rejection of the membrane was then studied through an ultrafiltration experiment using an aqueous solution containing 1000 ppm Bovine Serum Albumin (BSA) as the feed solution. Table 9 depicts the BSA rejections the membranes prepared using different PEG concentrations. As can be seen, the use of less concentration of PEG as the additive resulted in an increase in BSA rejection. This result is in accordance with the result of the SEM analysis and the analysis of the porosity and pore size which showed a decrease of the pore size when less concentration of PEG was used as described above. A high rejection of 90 % was achieved using the membrane 4000 – 1.25 that used a low concentration of PEG. The permeate fluxes of the membranes using the BSA solution as the feed are shown in Fig. 16. The permeate flux decline with time due to fouling was observed, however the membrane 4000 – 2 still exhibited the highest permeate flux.

In addition to the finding of this work, it has been known that ultrafiltration membranes have great potential for various applications such as removal of organics, microorganisms, particulates and colloidal material from water and wastewater, however ultrafiltration membranes have a drawback because of the permeate flux decline with time due to fouling. Many studies have been done to minimize the fouling problem such as backwash operation, cleaning, optimization of chemical/operational conditions, etc. [37–39]. Such kinds of methods to minimize fouling are very important for the future application of the membranes developed in this work. Moreover, besides flux and selectivity, the chemical resistance and the mechanical resistance of a membrane are very important for the industrial application as studied by Quallal et al. [40]. PET films have been known to have a good chemical resistance against chemical substances such as hydrocarbons, alcohols, ketones, ethers, esters. They also show a good chemical resistance against acids such as hydrochloric acids (10 %), sulfuric acids (20 %), nitric acids (10 %), and against low concentration of alkalies such as sodium hydroxides (2%) and ammonium hydroxides (2%) [41]. Moreover, their outstanding mechanical resistance such as tensile strength, tensile modulus of elasticity and elongation of break, make PET films suitable for many applications as reported in many studies [42,43]. The excellent chemical and mechanical resistance of PET makes the ultrafiltration membranes developed from PET to have great potential for various industrial applications.

4. Conclusion

Ultrafiltration membranes were developed from used polyethylene terephthalate (PET) bottles using phenol as the solvent and polyethylene glycol (PEG) as the additive. The results of the microstructure analysis using SEM and the analysis of the porosity and pore size showed that the pore size of the PET membranes could be controlled by varying the type of non-solvent, the PEG molecular weight and the PEG concentration. By using various types of non-solvents, namely water-ethanol, water-*n*-propanol or water-*n*-butanol, the pore size and the permeate flux of the membrane increased in the following order: water-ethanol < water-*n*-propanol < water-*n*-butanol. The hydrophilicity and the permeate flux of the membranes could also be increased by increasing the molecular weight and the concentration of PEG in the casting solution. High rejection values of Bovine Serum Albumin (BSA) of 90 % and 91 % were achieved using the membrane 4000 – 1.25 and the membrane 400 – 2, respectively. This result showed that the utilization of used PET bottles as a raw material to fabricate the ultrafiltration membranes has great potential to contribute in the recycling of PET bottles to produce a higher-grade product.

CRediT authorship contribution statement

Samuel P. Kusumocahyo: Conceptualization, Methodology, Supervision, Writing - review & editing. **Syarifa K. Ambani:** Investigation, Visualization. **Sylvia Kusumadewi:** Investigation, Visualization. **Hery Sutanto:** Data curation, Formal analysis. **Diah I. Widiputri:** Validation. **Irvan S. Kartawiria:** Validation.

Declaration of Competing Interest

The authors declare that they have no known competing financial interests or personal relationships that could have appeared to influence the work reported in this paper.

Acknowledgment

This work has been financially supported by the Ministry of Research, Technology and Higher Education of the Republic of Indonesia through the WCR research grant program 2019/2020.

References

[1] B. Huang, Q. Liu, J. Caro, A. Huang, J. Membr. Sci. 455 (2014) 200–206.
[2] S.P. Kusumocahyo, T. Ichikawa, T. Shinbo, T. Iwatsubo, M. Kameda, K. Ohi, Y. Yoshimi, T. Kanamori, J. Membr. Sci. 253 (1-2) (2005) 43–48.

[3] S.P. Kusumocahyo, K. Sumaru, T. Kanamori, T. Iwatsubo, T. Shinbo, J. Membr. Sci. 230 (1-2) (2004) 171–174.
[4] Y. Ohta, K. Akamatsu, T. Sugawara, A. Nakao, A. Miyoshi, S.-I. Nakao, J. Membr. Sci. 315 (1-2) (2008) 93–99.
[5] K. Xu, C. Yuan, J. Caro, A. Huang, J. Membr. Sci. 511 (2016) 1–8.
[6] H.-R. Xie, C.-H. Ji, S.-M. Xue, Z.-L. Xu, H. Yang, X.-H. Ma, Sep. Purif. Technol. 206 (2018) 218–225.
[7] H. Yan, J. Li, H. Fan, S. Ji, G. Zhang, Z. Zhang, J. Membr. Sci. 481 (2015) 94–105.
[8] S.P. Kusumocahyo, M. Sudoh, J. Eng. Technol. Sci. 48 (1) (2016) 99–110.
[9] N. Kosinov, J. Gascon, F. Kapteijn, E.J.M. Hensen, J. Membr. Sci. 499 (2016) 65–79.
[10] S.K. Hubadillah, M.H.D. Othman, T. Matsuura, A.F. Ismail, M.A. Rahman, Z. Harun, J. Jaafar, M. Nomura, Ceramics Int. 44 (2018) 4538–4560.
[11] C. Liu, H. Mao, J. Zheng, S. Zhang, J. Membr. Sci. 530 (2017) 1–10.
[12] B. Pulido, S. Chisca, S.P. Nune, J. Membr. Sci. 564 (2018) 361–371.
[13] F. Gholami, S. Zinadini, A.A. Zinatizadeh, A.R. Abbasi, Sep. Purif. Technol. 194 (2018) 272–280.
[14] T. Ahmad, C. Guria, A. Mandal, J. Membr. Sci. 564 (2018) 859–877.
[15] S. Rajesh, Z.V.P. Murthy, Quim. Nova 37 (4) (2014) 653–657.
[16] M.V. Zdorovets, A.B. Yeszhanov, I.V. Korolkov, O. Güven, S.S. Dosmagambetova, D.I. Shlimasa, Zh.K. Zhatkanbayeva, I.S. Zhidkov, P.V. Kharkin, V.N. Gluchshenko, D.A. Zheltov, N.A. Khlebnikov, I.E. Kuklin, Biol. Sci. 118 (2020) 103128.
[17] I.V. Korolkov, A.B. Yeszhanov, M.V. Zdorovets, Y.G. Gorin, Olgun Güven, S.S. Dosmagambetova, N.A. Khlebnikov, K.V. Serkov, M.V. Krasnopyorova, O.S. Milts, D.A. Zheltov, Sep. Pur. Tech. 227 (2019) 115694.
[18] I.V. Korolkov, A.A. Mashentseva, Olgun Güven, Y.G. Gorin, M.V. Zdorovets, Rad. Phys. Chem. 151 (2018) 141–148.
[19] Nace T., Forbes 2017, Jul 26, https://www.forbes.com/sites/trevornace/2017/07/26/million-plastic-bottles-minute-91-not-recycled/.
[20] F. Welle, The Facts About PET, (2018) https://www.efbw.org/fileadmin/user_upload/documents/Publications/Factsheet_The_facts_about_PET_Dr._Frank_Welle_2018.pdf.
[21] L. Bartolome, M. Imran, B.G. Cho, W.A. Al-Masry, D.H. Kim, IntechOpen, (2012), https://doi.org/10.5772/33800 https://www.intechopen.com/books/material-recycling-trends-and-perspectives/recent-developments-in-the-chemical-recycling-of-pet.
[22] N.A.A. Hamid, A.F. Ismail, T. Matsuura, A.W. Zularisam, W.J. Lau, E. Yuliwati, M.S. Abdullah, Desal. 273 (2011) 85–92.
[23] J.H. Li, Y.Y. Xu, L.P. Zhu, J.H. Wang, C.H. Du, J. Membr. Sci. 326 (2) (2009) 659–666.
[24] T. Wu, B. Zhou, T. Zhu, J. Shi, Z. Xu, C. Hu, J. Wang, RSC Adv. 5 (2015) 7880–7889.
[25] J.F. Li, Z.L. Xu, H. Yang, L.Y. Yu, M. Liu, Appl. Surf. Sci. 255 (9) (2009) 4725–4732.
[26] H. Hua, N. Li, L. Wu, H. Wong, G. Wu, Z. Yuan, X. Lin, L. Tang, J. Environ. Sci. China (China) 20 (2008) 565–570.
[27] N. Cao, X. Yang, Y. Fu, J. Food Hydrocoll. 23 (3) (2009) 729–735.
[28] H.J. Oh, B.D. Freeman, J.E. McGrath, C.J. Ellison, S. Mecham, K.-S. Lee, D.R. Paul, Polym. 55 (6) (2014) 1574–1582.
[29] S. Wongchitphimon, R. Wang, R. Jiraratananon, L. Shi, C.H. Loh, J. Membr. Sci. 369 (1–2) (2011) 329–338.
[30] A. Idris, N.M. Zaina, M.Y. Noordin, Desal. 207 (1–3) (2007) 324–339.
[31] Y. Liu, G.H. Koops, H. Strathmann, J., Membr. Sci. 223 (2003) 187–199.
[32] A.A. El-Saftawy, A. Elfalaky, M.S. Ragheb, S.G. Zakhary, Rad. Phys. Chem. 102 (2014) 96–102.
[33] I. Donelli, P. Taddei, P.F. Smet, D. Poelman, V.A. Nierstrasz, G. Freddi, Biotechnol. Bioeng. Symp. 103 (5) (2009) 845–856.
[34] A. Mollahosseini, A. Rahimpour, M. Jahamshahi, M. Peyravi, M. Khavarpour, Desal. 306 (2012) 41–50.
[35] R. Mahendran, R. Malaisamy, D. Mohan, European Polym. J. 40 (3) (2004) 623–633.
[36] M.T.M. Pendergast, J.M. Nygaard, A.K. Ghosh, E.M.V. Hoek, Desal. 261 (3) (2010) 255–263.
[37] K. Katsoufidou, S.G. Yiantsios, A.J. Karabelas, J., Membr. Sci. 266 (2005) 40–50.
[38] H. Lee, G. Amy, J. Cho, Y. Yoon, S.-H. Moon, I.S. Kim, Wat. Res. 35 (14) (2001) 3301–3308.
[39] H. Chang, H. Liang, F. Qu, J. Ma, N. Ren, G. Li, J. Env. Sci. 43 (2016) 177–186.
[40] H. Quallal, M. Azrour, M. Messaoudi, H. Moussout, L. Messaoudi, N. Tijani, J. Env. Chem. Eng. 8 (2) (2020) 103668.
[41] Polyguard, Technical Bulletin – Chemical Resistance of PET/polyester Films, (2015) https://www.polyguardproducts.com.
[42] T. Horvath, M. Kalman, T. Szabo, K. Roman, G. Zsoldos, M.S. Szabone Kollar, IOP Conf. Ser.: Mater. Sci. Eng. 426 (2018) 012018.
[43] Y. Bin, K. Oishi, K. Yoshida, M. Matsuo, Polym. J. 36 (11) (2004) 888–898.